Directional tuning for eye and arm movements in overlapping regions in human posterior parietal cortex

Magri, Caterina; Fabbri, Sara; Caramazza, Alfonso; Lingnau, Angelika

Published in:
Neuroimage

DOI:
10.1016/j.neuroimage.2019.02.029

Publication date:
2019

Accepted Manuscript

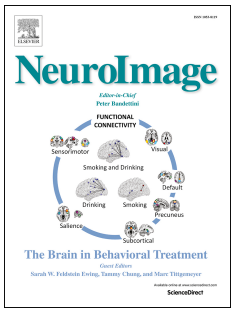

Directional tuning for eye and arm movements in overlapping regions in human posterior parietal cortex

Caterina Magri, Sara Fabbri, Alfonso Caramazza, Angelika Lingnau

PII: S1053-8119(19)30123-5

DOI: https://doi.org/10.1016/j.neuroimage.2019.02.029

Reference: YNIMG 15634

To appear in: *NeuroImage*

Received Date: 15 November 2018

Revised Date: 6 February 2019

Accepted Date: 11 February 2019

Please cite this article as: Magri, C., Fabbri, S., Caramazza, A., Lingnau, A., Directional tuning for eye and arm movements in overlapping regions in human posterior parietal cortex, *NeuroImage* (2019), doi: https://doi.org/10.1016/j.neuroimage.2019.02.029.

Directional tuning for eye and arm movements in overlapping regions in human posterior parietal cortex

Caterina Magri[1,2,3], Sara Fabbri[1,4], Alfonso Caramazza[1,3], & Angelika Lingnau[1,2,5]

[1]*Center for Mind/Brain Sciences (CIMeC), University of Trento, Italy*

[2] *Department of Cognitive Science, University of Trento, Italy*

[3] *Department of Psychology, Harvard University, Cambridge, MA, USA*

[4] *Department of Experimental Psychology, Faculty of Behavioural and Social Sciences, University of Groningen, The Netherlands*

[5] *Department of Psychology, Royal Holloway University of London, UK*

Authors contribution:

- Conception and design of work: Angelika Lingnau, Alfonso Caramazza
- Data collection: Sara Fabbri, Caterina Magri
- Data analysis and interpretation: Caterina Magri, Sara Fabbri, Angelika Lingnau
- Drafting and revision of the article: Caterina Magri, Sara Fabbri, Angelika Lingnau, Alfonso Caramazza

Corresponding author:

Prof. Dr. Angelika Lingnau
Department of Psychology
University of Regensburg
Universitätsstrasse 31
93040 Regensburg
Tel. ++49-941 943 3868
Fax ++49-941 943 3233
Email: angelika.lingnau@psychologie.uni-regensburg.de

Keywords: directional tuning, arm movements, saccades, Representational Similarity Analysis, posterior parietal cortex

ABSTRACT

A network of frontal and parietal regions is known to be recruited during the planning and execution of arm and eye movements. While movements of the two effectors are typically coupled with each other, it remains unresolved how information is shared between them. Here we aimed to identify regions containing neuronal populations that show directional tuning for both arm and eye movements. In two separate fMRI experiments, the same participants were scanned while performing a center-out arm or eye movement task. Using a whole-brain searchlight-based representational similarity analysis (RSA), we found that a bilateral region in the posterior superior parietal lobule represents both arm and eye movement direction, thus extending previous findings in monkeys.

HIGHLIGHTS

- Directional tuning in superior parietal lobule (SPL) for arm and eye movements
- Overlapping representations for both effectors in posterior SPL
- Underlying patterns of activation do not generalize across effectors

1. INTRODUCTION

To plan and perform visually guided prehension movements, we need to integrate movement information between eyes and arms. In addition to effector-specific information about the direction of a movement, movement direction thus also needs to be represented in an effector-independent format.

Neural populations tuned for *arm movement direction* have been found in monkey primary motor cortex (M1; Georgopoulos et al. 1986, 1982), premotor cortex (PM) and in several parietal areas (Caminiti et al., 1991; Johnson et al. 1996; Battaglia-Mayer et al. 2001; Stevenson et al. 2011; for a review, see Mahan and Georgopoulos 2013). Likewise, directionally tuned neuronal populations have been identified in human M1, premotor cortex and parietal cortex (Eisenberg et al. 2010; Fabbri et al. 2010, 2014).

Monkey lateral intraparietal area (LIP) is known to be involved in the planning and execution of *saccades* (Gnadt and Andersen 1988; Snyder et al. 1997; Zhang and Barash 2000). Moreover, neurons in the frontal eye fields (FEF) have been shown to be sensitive both to the direction and amplitude of saccadic eye movements and seem to follow a topographic organization (Bruce et al. 1985). In humans, putative LIP regions have been identified during visually guided saccades which also show topographical maps for memorized targets during delayed saccades and spatial memory tasks (Sereno et al., 2001; Schluppeck et al., 2005; Kastner et al., 2007).

Neurons in monkey superior parietal areas V6A, PEc and 7m have been observed to combine retinal-, eye- and arm-related signals in a spatially congruent way (Battaglia-Mayer et al. 2001, 2000): these neurons discharge during eye and arm movements performed in a segment of similar directions, referred to as *global tuning field*. Following these results, it has been suggested that the global tuning field serves the function of combining eye- and arm-related information in a directionally congruent way, therefore allowing a representation of movement direction independent from the effector (Battaglia-Mayer et al. 2001). In line with this interpretation, reversible inactivation of bilateral superior parietal area 5 in monkeys interfered with online control of not only arm but also eye movements (Battaglia-Mayer et al. 2013).

In humans, an assessment of effector preference in topographically organized maps in the posterior part of the human intraparietal sulcus (pIPS) suggested that this region contains information related to the movement of both eyes and arms (Levy et al. 2007). Using multivariate pattern analysis of fMRI data, Gallivan et al. (2011)

were able to decode from patterns of activation obtained in left pIPS and bilateral mIPS whether an upcoming movement was going to be directed to a target on the left or the right side, both within the same effector (eye or arm) and across effectors.

While these neuroimaging studies showed that posterior parietal cortex (PPC) contains detailed representations of the target location for both eye and arm movements, it remained unclear whether this region contains directionally tuned neuronal populations irrespective of the effector (eye or arm), in line with the global tuning fields identified in monkeys. Areas with such properties would constitute good candidates as a site of integration of spatial information across effectors. To identify areas with such properties in humans, we tested the same set of participants in two separate fMRI experiments that required center-out arm (Experiment 1) or eye movements (Experiment 2). Data for Experiment 1 were collected as part of another study focusing on reach direction and grip type (Fabbri et al. 2014). To identify regions that are sensitive to either arm or eye movement direction (or both) we conducted a searchlight-based Representational Similarity Analysis (RSA; Kriegeskorte et al. 2006) separately for both experiments and examined the overlap between the two resulting maps.

2. MATERIAL AND METHODS

2.1 Experimental design

2.1.1 Participants. Fourteen right-handed participants (seven females; age range: 20-52 years) were scanned in two separate experiments, carried out in separate scanning sessions, while performing a center-out reaching or saccade task. Experimental procedures were approved by the ethics committee for research involving human participants at the University of Trento, Italy.

2.1.2 Reaching task. During the reaching task, participants performed a center-out, reach-to-grasp task on a device attached to their chest. The device consisted of 5 half-spheres of polystyrene (3 cm diameter) glued on a black plastic surface (see Figure 1A). These spheres were placed at five equidistant positions on an invisible semicircle (8 cm radius) and at the center of the semicircle. The orientation of an arrow presented at the center of the screen visible to the participant via a mirror attached to the head coil (for details, see *Setup*) indicated the reach direction (0, 45, 90, 135 and 180°, where 0° corresponds to rightward movements), whereas its color specified the type of grip (whole-hand grip, pincer grip or touch; Figure 1B,C; for details, see Fabbri et al., 2014). The arrow appeared for 2 seconds (s) followed by an inter-trial interval (ITI) of 1s. At the beginning of each trial, participants maintained the index finger on the sphere at the center of the circle. Once the arrow appeared, participants had to perform a reach-to-grasp movement toward one of the five spheres and return the index finger to the central position. Overall, there were 3 (movement types) x 5 (directions) conditions. Note that we varied grip type to investigate a separate question (see Fabbri et al., 2014) unrelated to the current study. Since here we were interested in finding overlapping representations of arm and eye movements, irrespective of their types and directions, we collapsed across the three different grip types.

2.1.3 Saccade task. Similar to the reaching task, an arrow appeared for 2s followed by an ITI of 1s. Participants had to maintain their gaze at fixation until the appearance of the arrow. Once the arrow appeared, participants performed a center-out saccade toward one of the eight targets and returned to the central fixation point. Targets were

located at equidistant positions around the fixation point at 0, 45, 90, 135, 180, 225, 270, and 315° (where 0° corresponds to rightward movements) on an invisible circle with a diameter of 400 pixels (visual angle: 5.6°; see Figure 1C,E). Throughout the task, participants maintained their right hand at rest on their right side.

Note that the visual cues were different for the saccade and for the reaching task. In the reaching task, an upward arrow indicated a downward reach (see Figure 1B, C). Instead, in the saccade task, an upward arrow indicated an upward saccade (see Figure 1D,E). Thus, saccades and reaches were performed towards different points in space.

2.1.4 Setup. During both tasks, stimuli were back-projected onto a screen by a liquid-crystal projector (OC EMP 7900; Epson Nagano, Japan) at a frame rate of 60 Hz and a screen resolution of 1,280 x 1,024 pixels (mean luminance: 109 cd/m^2). Participants were scanned in a conventional configuration, i.e. horizontally, without tilting the head towards the body, precluding a direct view of their own arms (see also Ariani et al., 2015; Fabbri et al. 2010; 2012; 2014).

Participants viewed the stimuli binocularly through a mirror above the head coil. The screen was visible as a rectangular aperture of 17.5 x 14.3 degrees. Visual stimulation was controlled by ASF (Schwarzbach 2011) based on the MATLAB Psychtoolbox-3 for Windows (Brainard 1997; Pelli 1997). For the reaching task, the visual appearance of the arrow instructing the movement on each trial was varied in order to reduce visual similarity between trials (see also Fabbri et al. 2010, 2012, 2014). Arrow width and length were varied randomly from 0.41° to 1.22° in steps of 0.405°. The x- and y-centered coordinates of the arrow were jittered in a range of +/- 0.07° in steps of 0.035°.

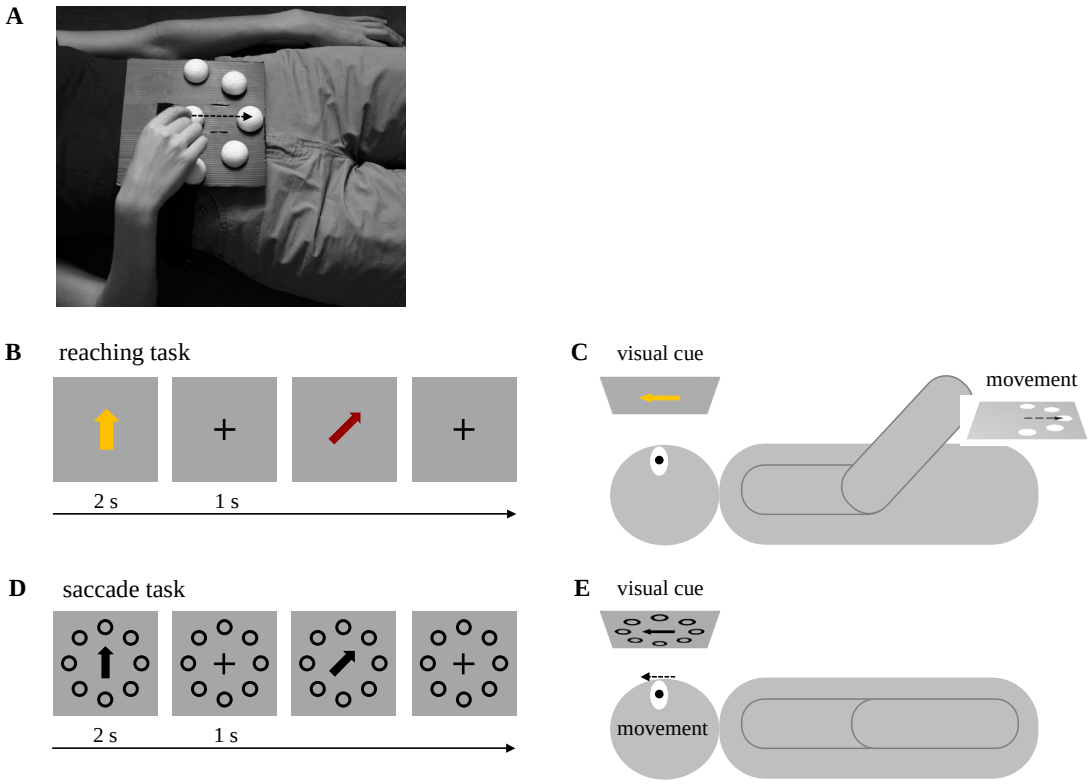

[single column fitting image]

Figure 1. Task and Apparatus. A: *The device used to perform the reaching task (adapted from Fabbri et al., 2014).* ***B****: Illustration of the reaching task. Participants were instructed to perform center-out reach-to-grasp movements toward one of five possible reach directions (0, 45, 90, 135 and 180°, where 0 corresponds to a rightward movement) as indicated by the orientation of an arrow presented at the center of the screen. In this example trial, the first arrow is pointing in the 90° direction and the second one in the 45° direction.* ***C****: Schematic of the spatial layout for the reaching task. In this example, an upward arrow (90° direction) led to a downward reach.* ***D:*** *Illustration of the saccade task. Participants were instructed by the orientation of an arrow presented at fixation (enlarged in this figure for ease of visualization) to perform a saccade from the central fixation point toward one of eight possible saccade directions (0, 45, 90, 135, 180, 225, 270 and 315°).* ***E****: Schematic of the spatial layout for the saccade task. In this example, an upward arrow (90° direction) led to an upward saccade.*

2.1.5 Instruction and Training. Before entering the scanner, participants were familiarized with the task and the positions of the targets and performed a short practice session. Participants were instructed to perform center-out arm or eye movements, returning to the central position within a constant time window of 2s corresponding to the time of the appearance of the arrow.

2.1.6 Design. Both the reaching and the saccade experiment consisted of 12 event-related runs. For the reaching experiment, each run consisted of 75 experimental trials and 10 null trials. Each of the 15 conditions (5 directions x 3 movement types) was repeated 5 times in a run, for a total of 60 repetitions for each condition for each participant. For the saccade task, each run consisted of 80 experimental trials and 10 null trials, for a total of 80 repetitions for each condition for each participant.
During null trials, participants were instructed to remain still while keeping their eyes at fixation. In both experiments, the order of experimental and null trials was randomized.

2.1.7 Data acquisition. fMRI data were acquired using a 4T Bruker MedSpec Biospin MR scanner and an 8-channel birdcage head coil. Functional images were acquired with a T2*-weighted gradient-recalled echo-planar imaging (EPI) sequence. Before each functional scan, an additional scan was performed to measure the point-spread function (PSF) of the acquired sequence, which served for correction of the distortion expected with high-field imaging (Zaitsev et al. 2004). 34 slices were acquired in ascending interleaved order, slightly tilted to run parallel to the calcarine sulcus (TR [time to repeat]: 2000ms; voxel resolution: 3x3x3 mm; TE (echo time): 33ms; flip angle (FA): 73°; field of view (FOV): 192 x 192 mm; gap size: 0.45 mm). Each participant completed 12 runs of 146 volumes each for the reaching task and 12 runs of 165 volumes each for the saccade task. To be able to co-register the low-resolution functional images to a high-resolution anatomical scan, a T1 weighted anatomical sequence (MP-RAGE; voxel resolution: 1x 1 x 1 mm; FOV: 256 x 224 mm; GRAPPA acquisition with an acceleration factor of 2; TR: 2700ms, inversion time (TI), 1020ms; FA: 7°) was acquired in both sessions.

2.2 fMRI data analysis

Data analysis was performed using BrainVoyager QX 2.6 (Brain Innovation), the BVQX Toolbox (http://support.brainvoyager.com/available-tools/52-matlab-tools-bvxqtools.html) and custom programs written in MATLAB (Mathworks).

2.2.1 Preprocessing. Distortion correction was applied on the basis of the PSF data acquired before each EPI scan. This procedure corrects for distortions in geometry and intensity in the EPI images (Zeng and Constable 2002). The first 4 volumes were removed to avoid T1-saturation, and 3D motion correction was performed with trilinear interpolation using the first volume as reference. Finally, slice timing correction was performed. Functional data were temporally high-pass filtered using a cut-off frequency of 3 cycles per run. To correct for head motion, the first volume of the reference run was aligned to the anatomical scan and the remaining functional runs were aligned to the reference run as part of 3D motion correction.

2.2.2 Masking and segmentation. For each participant, the native space anatomical scan acquired during the reaching task session was transformed to the ACPC-transformed anatomical scan acquired during the saccade task session. Next, the two aligned anatomical scans were transformed into Talairach space and averaged to improve the quality of cortex segmentation. To produce a gray matter mask, we segmented the border between gray and white matter of the averaged anatomical data. The resulting mesh was expanded -1 to 3 mm from the vertex along the vertex normals. The following analyses were performed within this resulting gray matter mask.

2.2.3 Cortex-based alignment. To improve the spatial correspondence between participants, we carried out cortex-based alignment of the individual statistical maps (Fischl et al. 1999). Cortex-based alignment was performed in an iterative procedure by using the curvature information of the individual segmented and inflated hemispheres of all participants, separately for the left and right hemisphere. The iterative process progresses from more smoothed to less smoothed curvature maps, resulting in a correspondence mapping which relates each vertex of the group-aligned sphere to each vertex of the individual sphere. These correspondence mappings were used to transform the individual statistical maps to a group-aligned map. Furthermore, for ease of

visualization, the inflated left and right hemispheres representing the average curvature maps for all the participants were reconstructed.

2.2.4 GLM. Separately for each experiment, condition, and run, we z-transformed time courses extracted from each voxel within the gray matter mask. Next, we computed a RFX GLM analysis. For the reaching experiment, we used the factors *reach direction* (0, 45, 90, 135, 180°) and *movement type* (touch, pincer-grip, whole-hand grip) for a total of 5 x 3 =15 predictors. For the saccade experiment, we used the factor *saccade direction* (0, 45, 90, 135, 180, 225, 270 and 315°). For both experiments, we added six additional parameters resulting from 3D motion correction (x, y, z translation and rotation) as predictors of no interest. Each predictor time course was convolved with a dual-gamma hemodynamic impulse response function (Friston et al. 1998), and the resulting reference time courses were used to fit the signal time course of each voxel.

Since we were interested in investigating the direction of arm movement regardless of movement type, we collapsed beta weights across movement type (whole-hand grip, pincer grip, touch) for the reaching experiment. Furthermore, we restricted the analysis to those directions covered in both experiments (i.e., directions from 0°, corresponding to a rightward movement, to 180°, corresponding to a leftward movement).

2.2.5 RSA Searchlight. We were interested in exploring which brain areas contain directionally tuned neuronal populations. We reasoned that patterns of voxels in such areas should be more similar for movements performed in similar directions, and that this similarity should decrease with increasing angular distance between reaching movements (see also Eisenberg et al., 2010; Fabbri et al., 2014). To identify areas with such properties, we ran a representational similarity analysis (RSA; Kriegeskorte et al., 2008). RSA uses multivariate pattern analysis (Haxby et al., 2001) to quantitatively relate neural data with predicted data derived from different models and/or other types of data (e.g. behavioral measurements). Here, we employ RSA to identify neural patterns for directionally tuned neuronal populations.

Based on results from previous studies (Georgopoulos et al., 1982, 1986; Eisenberg 2010, Fabbri 2014), we constructed a *target matrix*, i.e. a similarity matrix we expected to obtain within a region that encoded directional tuning information. In this target matrix (see Figure 2A), rows and columns represent the expected similarity in

the patterns of activation between data acquired during odd (rows) and even runs (columns) for the five different movement directions. Similarity is expected to be high along the diagonal, i.e. for data from odd and even runs with identical movement directions. Similarity is expected to gradually decrease with increasing angular distance between the movement direction in odd and even runs. We built the target matrix by using a Gaussian function ($\mu = 0$, $\sigma = 0.3$) and computing its probability density function for x = -1:0.25:1, corresponding to angular distances of -180:45:180. The resulting values were then assigned to the target matrix with the following mapping: along the diagonal we assigned the values of the function at x = 0, in the lower left triangle of the matrix we assigned the values corresponding to the left part of the curve, and in the upper left triangle of the matrix we assigned values corresponding to the right part of the curve (Figure 2A).

To determine the observed matrix (Figure 2B), we employed a searchlight analysis (Kriegeskorte et al., 2006). In brief, separately for each participant, for each voxel contained in the gray-white matter mask, we identified a sphere (radius: 7mm) around that voxel and extracted the β-estimates for each of the five different movement directions, separately for the two experiments and the different runs, for all the voxels included in that sphere. The sphere contained an average of 46.11 voxels ($\sigma = 9.44$). Note that the number of voxels contained in the searchlight varied depending on the position of the central voxel. If, for example, the voxel selected as the center was located near the border between gray and white matter, the number of neighbors contained in the searchlight was smaller. To build the observed matrix, within each searchlight, β-estimates for the five different directions and the two experiments were averaged across odd and even runs. Next, separately for each searchlight, data were normalized by subtracting the grand mean response across conditions from each voxel, separately for odd and even runs (Haxby et al. 2001). This normalization was performed to eliminate differences in activation between voxels. For each experiment, this produced two vectors of β-estimates for each of the five directions. Next, we computed the correlation coefficient *r* between the vectors of β-estimates for each pairwise comparison of movement directions from odd and even runs (see Figure 2B), separately for the reaching and the saccade experiment.

A visualization of the directional tuning of the observed matrix can be observed in Figure 2C (see legend for details). To test whether a neural population within a searchlight was directionally tuned, we computed the correlation coefficient between

the neural similarity matrix and the target matrix and assigned the resulting value to the central voxel of the searchlight. The results of the searchlight-based RSA were Fisher-transformed and stored in a volumetric map, separately for each participant and experiment. These maps were projected to the surface, and the resulting individual surface maps were group-aligned, using the correspondence mapping obtained from cortex-based alignment, separately for the two experiments.

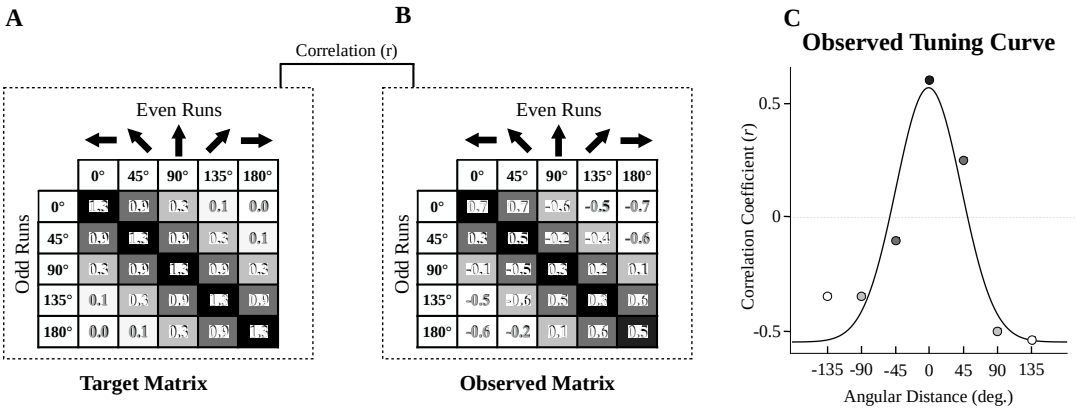

[1.5 column fitting image]

Figure 2. Target and Observed Matrices. ***A****: The target matrix was constructed using a Gaussian function with μ=0 and σ=0.3 (see Methods for details).* ***B****: Observed matrix: a matrix of correlation values between patterns of brain activation for each possible combination of movement directions during odd and even runs. Data for this visualization result from a searchlight located in the central sulcus for the arm movement experiment of one representative participant.* ***C****: RSA-based directional tuning curve, plotting the correlation values depicted in the Observed Matrix (B) as a function of the angular distance between directions. For example, the point at the center of the plot, at zero angular distance, corresponds to the average across all correlations along the diagonal. The value at an angular difference of -45° corresponds to the average across all angular differences between odd and even runs of -45°, and so forth. A Gaussian function was fit along the obtained values for ease of visualization.*

2.2.7 Group Maps. We performed group statistics on the cortically aligned correlation maps by performing a t-test of all individual searchlight maps versus zero, separately for the two experiments. We corrected the two resulting statistical maps for multiple comparisons using false discovery rate (FDR; Benjamini & Yekutieli, 2001) correction (q[FDR] < 0.01) and superimposed the two maps (Figure 3). Furthermore, for

ease of visualization, we thresholded maps by retaining voxels with the top 5, 10 and 15% t-values **(**Figure 4; see also Fabbri et al., 2014).

2.2.8 Directional tuning for overlapping regions.

To visualize directional tuning within and across effectors in the bilateral region in SPLp identified by the whole-brain searchlight analysis, we computed the pairwise correlation coefficient between β-estimates for each possible combination of movement directions between odd and even runs, within and across effectors. The resulting correlation values were Fisher-transformed and, separately for each participant, averaged across pairwise comparisons with similar angular distances (0°, +/-45, +/-90 and +/-135°). Finally, we computed the mean of these values across participants and plotted the resulting values as a function of the angular distance between movements performed in odd and even runs within (Figure 5A,B) and across effectors (Figure 5C,D).

2.2.9 Data and code availability statement

Data not available/ The authors do not have permission to share data.

3. RESULTS

Directional tuning maps for reaching and saccadic eye movements can be seen in Figure 3 (q[FDR] < 0.01). Regions depicted in red correspond to voxels that contain directional tuning information for arm movements, regions depicted in blue contain directional tuning information for saccades; and voxels in which the two maps overlap, which thus contain both directional tuning information for arms and for saccades, are depicted in purple. As an inspection of Figure 3 reveals, the correlation map resulting from the reaching task is widespread, covering parietal, frontal and temporal regions, whereas the corresponding map resulting from the eye movement task and the overlap between the two is limited to the posterior parietal and occipital cortices.

For ease of comparison, Figure 4 shows the same correlation maps as those depicted in Figure 3, thresholded to retain voxels with the top 5, 10, and 15% t-values for each map (see also Fabbri et al., 2014).

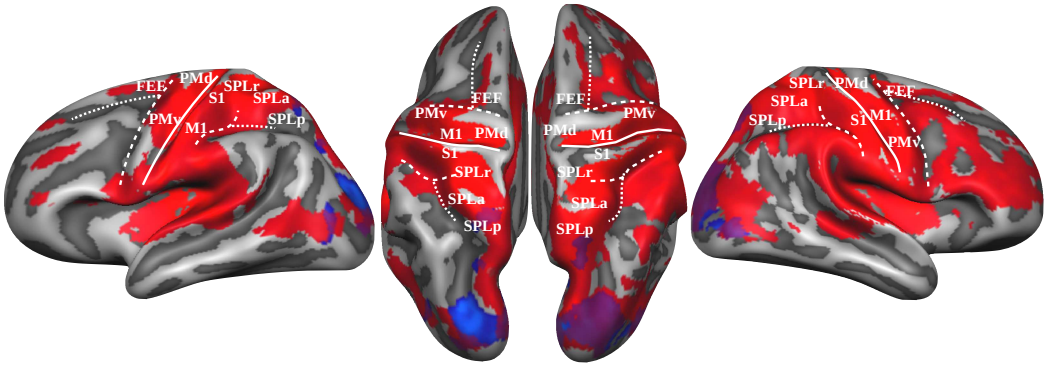

367 [1.5 column fitting image]

368 ***Figure 3. Searchlight-based RSA maps (FDR-corrected).*** *Maps of arm (red) and eye*
369 *(blue) movement directional tuning and their overlap (purple), corrected for multiple*
370 *comparisons (q[FDR] < 0.01). Visualized are only regions that extended beyond a*
371 *cluster size of 25mm^2. Minimum t-values were 4.79 for eye movements and 3.25 for*
372 *arm movement.*

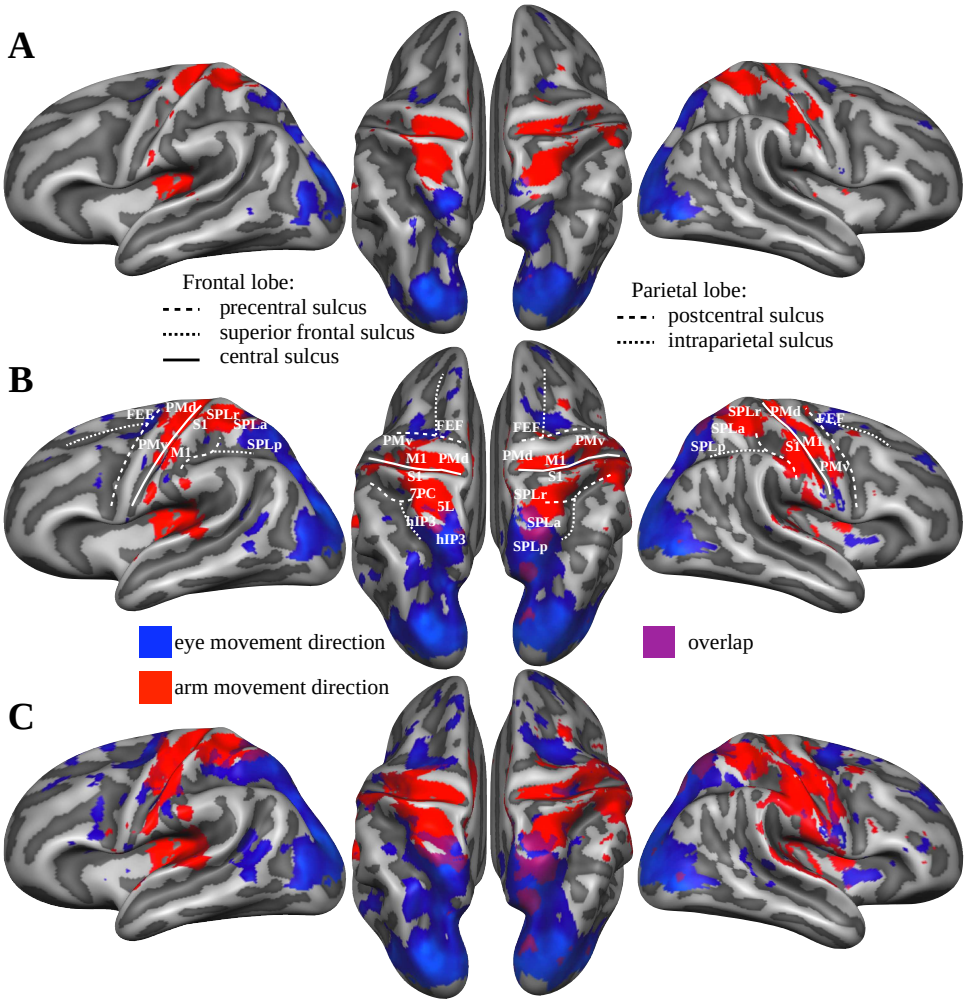

[1.5 column fitting image]

Figure 4. Searchlight-based RSA maps (top 5, 10, and 15% t-values). *Statistical maps depicting correlations between the target and observed matrix for eye (blue) and arm (red) movement direction. Maps are thresholded as to retain voxels with the top 5% (**A**), 10% (**B**) and 15% (**C**) of the highest t-values, separately for arm and eye movements. Thresholding at 5%, 10%, and 15% corresponded to minimum t-values of 7.4, 6.2 and 5.5 for arm movements, and to minimum t-values of 3.4, 2.4 and 1.9 for eye movements. FEF, frontal eye fields; dPM, dorsal premotor cortex; M1, primary motor cortex; S1, somatosensory cortex; SPLr, SPLa and SPLp correspond to the rostral, anterior and posterior portion of superior parietal lobule.*

3.1 Arm movement map

We obtained the highest t-values for directional tuning for reaching movements in primary motor (M1) and somatosensory (S1) cortex. Directional tuning information was also present in ventral (PMv) and dorsal (PMd) premotor cortex and, in the parie-

tal lobe, in rostral, anterior and posterior superior parietal lobule (SPLr, SPLa, SPLp; Figure 3 and 4; see Table 1 for corresponding Talairach coordinates).

3.2 Eye movement map

As can be observed from Figures 3 and 4, directional tuning for eye movements was present bilaterally in the occipito-temporal cortex and spread dorsally to the parietal cortex in SPLp, as well as in the vicinity of the FEF (Anderson et al. 2012; see Table 1 for Talairach coordinates for all regions mentioned). At more liberal thresholds, directional tuning information was also observed in SPLa and SPLr (Figure 4B,C).

3.3 Directional tuning for both effectors

An overlap between the two maps depicting directional tuning for arm and eye movements should reveal regions containing neuronal populations that are directionally tuned both for arm and eye movements. When both maps were FDR-thresholded ($q[FDR] < 0.01$; see Figure 3), we observed an overlap between the two maps bilaterally in SPLp. This region was also present, but located slightly more anteriorly, when thresholding the maps as to retain the voxels with the top 10 and 15% of the highest t-values (Figure 4B,C). In the left hemisphere, this region extended anteriorly to SPLa. In the right hemisphere, it extended more posteriorly and medially towards IPS (see Figure 3 and Table 1), largely corresponding to a region recently identified as being the homologue of monkey MIP and anterior LIP (Orban, 2016).

The two bilateral clusters in SPLp in which the searchlight-based RSA revealed directional tuning for both effectors might be due to two different underlying patterns of results. First, it is possible that both clusters contain directionally tuned populations for eyes and arms, but that the underlying patterns of activation differ between the two effectors. In this case, the corresponding tuning curve across effectors should be flat. Second, it is possible that both clusters contain directionally tuned populations for eyes and arms, and that the underlying patterns of activation are similar for the two effectors. In this case, we should obtain a tuning curve across effectors that is centered around an angular distance of 0°. To distinguish between these two alternatives, we plotted the directional tuning curves within (Figure 5A,B) and across effectors (Figure 5C,D) for the bilateral clusters in SPLp as observed in the FDR-corrected map in Figure 3. Note that these tuning curves are not independent from the RSA which aimed to identify directionally tuned areas; directional tuning was thus expected for both effectors. Indeed, within-effector directional tuning was present in the

overlapping region (Figure 5A,B). By contrast, the corresponding directional tuning for the cross-effector comparison showed little if any, as evidenced by an essentially flat curve in Figures 5C,D.

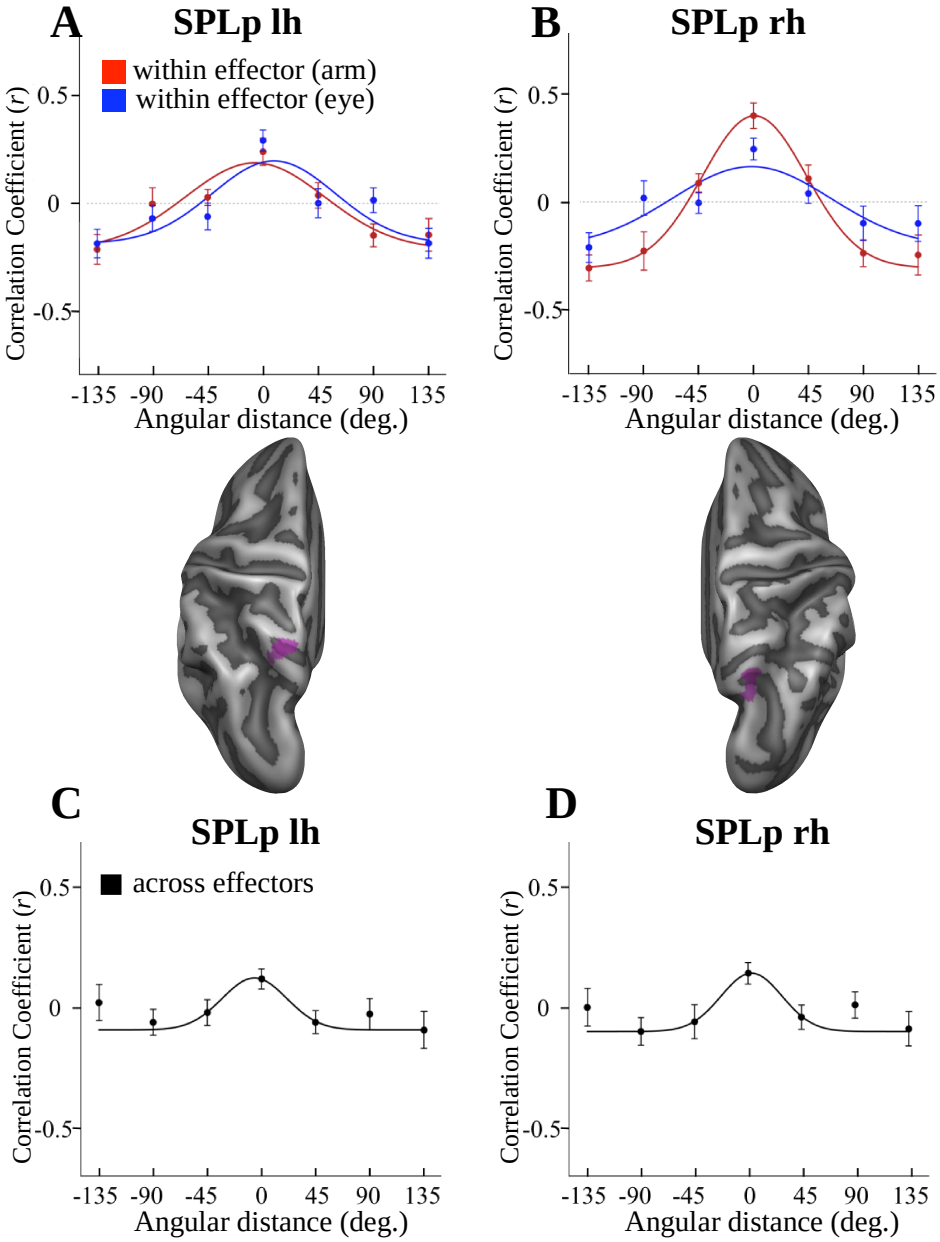

[1.5 column fitting image]

Figure 5: Directional tuning plots. *X-axis: angular distance between movement directions obtained within effector (A,B) and across effector (C,D). Y-axis: Fisher-transformed correlation values (r) between odd and even runs (A,B) and between the reaching and saccade task (C,D) as a function of the angular distance between movement directions.* ***A,B****: Within-effector correlations (red: arm, blue: eye) obtained from the overlapping area for left and right SPLp.* ***C, D****: Across-effector correlation obtained from left and right SPLp. The location of the overlapping region in SPLp, as visible in the FDR-corrected map in Figure 3, is shown superimposed on the seg-*

435 *mented and inflated left and right hemispheres reflecting the average gyral and sulcal*
436 *patterns across participants.*

As a sanity check, we plotted the within-effector directional tuning for a region along the central sulcus where only the arm movement map, but not the eye movement map, was present. As expected, we found directional tuning for the arm, but not for the eye (see Appendix, Figure A1).

To rule out that the searchlight analysis was driven by the main effect of the diagonal of the data matrix (see also Ritchie et al., 2017), we repeated the same analysis as before but removed the matrix diagonal from both target and observed matrices, thresholding the maps both with FDR correction (Figure 6A) and as to show the top 15% voxels with highest t-value (Figure 6B). As expected, the overall results were slightly weaker, but otherwise looked very similar to those obtained when the matrix diagonal was included, thus ruling out that the searchlight analysis results were driven by a main effect of the diagonal. When superimposing the outline of the bilateral area in SPLp where the directional information was present for both effectors to this map (see green outline in Figure 6A,B), arm and eye information is still present in these regions, although it does not appear to emerge for the eye movement map when FDR-thresholded.

Table 1

Region	x	y	z
FEF LH	-25	-11	51
FEF RH	21	-8	52
SPLr LH	-22	-44	56
SPLr RH	20	-46	54
SPLa LH	-23	-55	5657
SPLa RH	18	-55	56
SPLp LH	-13	-63	56
SPLp RH	20	-71	45

Table 1. *Talairach coordinates for exemplar regions showing directional tuning for arm movements, eye movements, or both. FEF, frontal eye fields; SPLr, rostral superior parietal lobule; SPLa, anterior superior parietal lobule; SPLp, posterior superior parietal lobule. For SPLp, the coordinates shown refer to the region of overlap for the FDR-thresholded arm and eye movement statistical maps depicted in Figure 3.*

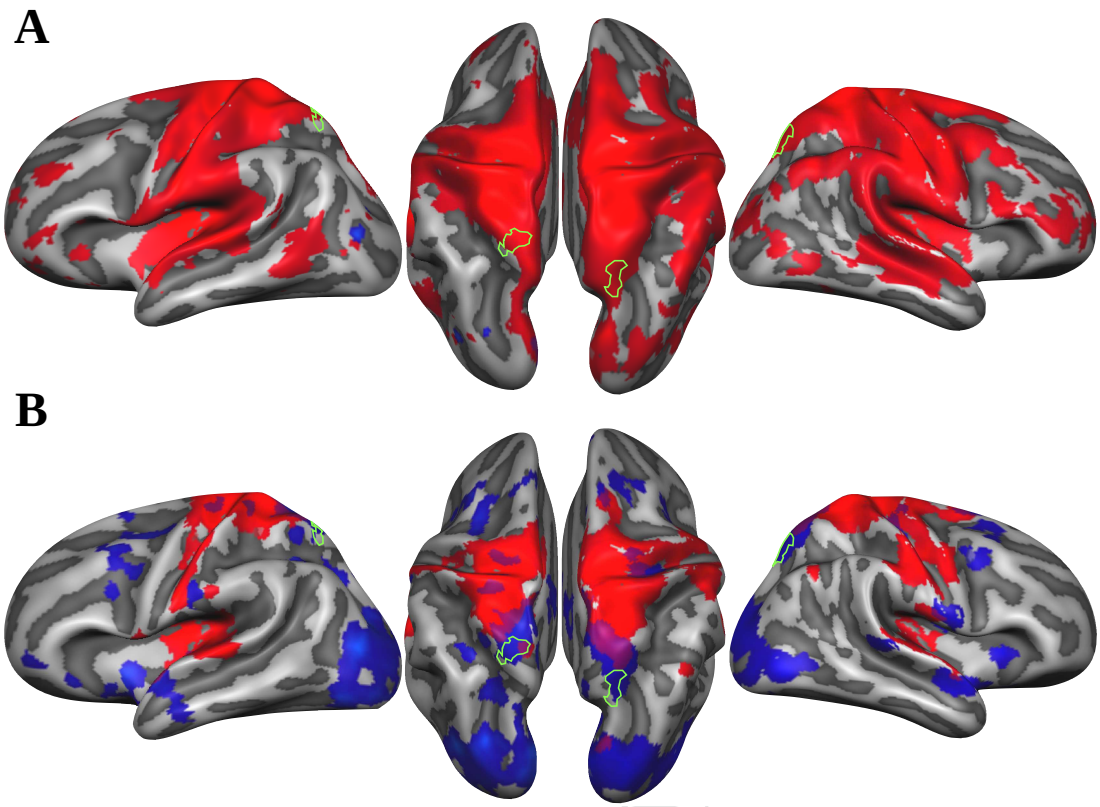

[1.5 column fitting image]

Figure 6. Searchlight-based RSA maps without matrix diagonal. *Directional tuning maps depicting correlations between the target and observed matrices for arm (red) and eye (blue) movement direction and their overlap (purple) after removing the matrix diagonal.* ***A)*** *Maps are thresholded to FDR [q]<0.05 for both maps.* ***B)*** *Maps are thresholded as to retain voxels with the top 15% of the highest t-values for each effector. This corresponded to a minimum t-value of 4.611 for the arm movement map and 1.856 for the eye movement map. Outline in green shows approximate location of the bilateral area in SPLp where directional information was present for both effectors. This region was selected from the FDR-corrected maps shown in Figure 3.*

4. DISCUSSION

Movements of the eyes and the arms need to be coordinated and integrated for efficient interactions with the environment. Here we aimed to identify regions in the fronto-parietal network that represent the direction of arm movements, eye movements, or both. Previous monkey and human studies identified effector-specific parietal regions involved during movement preparation and execution (Andersen and Cui 2009; Connolly et al. 2003; Scherberger and Andersen 2007; Sereno et al. 2001; Snyder et al. 1997). More recent studies additionally identified overlapping regions for eye and arm movements in rostral posterior parietal cortex (Leoné et al. 2014). In concordance with this second line of findings, an extensive review (Battaglia-Mayer et al. 2016) has recently documented the presence of cross-talk and connectivity between both frontal and parietal areas showing effector-preference, with SPL processing both saccades and hand-related signals. The present study extends the existing literature by not only identifying areas recruited for eye or arm movements in posterior SPL, but by additionally demonstrating the presence of two sets of overlapping neuronal populations that are tuned to the direction of eye and arm movements, respectively. However, we failed to obtain evidence for shared representations between the two effectors. In the following, we discuss these results in more detail.

Areas representing arm movement direction

As can be observed from the maps depicted in Figures 3 and 4, we obtained regions containing directionally tuned neuronal populations for arm movements bilaterally in PMd, PMv, M1, S1, SPLr, SPLa and SPLp. These observations are in agreement with previous monkey studies (Battaglia-Mayer et al. 2001; Georgopoulos et al. 1986, 1982; Johnson et al. 1996; Stevenson et al. 2011), and with human fMRI adaptation and multivariate pattern analysis studies (Eisenberg et al. 2010; Fabbri et al. 2010, 2012, 2014; Lingnau et al. 2012). Likewise, Barany et al. (2014) were able to decode both the direction of arm movements and the target location in SPL, supporting a role of this region in sensory-motor transformations. It should be noted that posterior parietal cortex in monkey and humans is modulated by wrist orientation (Fattori et al., 2009; Breveglieri et al., 2017; Monaco et al., 2011). Since participants in the current study were likely to rotate their hand to a certain degree to perform the task, sensitivity to wrist orientation may have contributed to the results we obtained in posterior parietal cortex.

Further, the guiding visual information was not presented in spatial alignment with the required motor output target. This might trigger additional processes required to spatially re-align the spatial target with the movement target, which are not required during normal reaching conditions. SPL has been observed to preserve directional motor encoding in the presence of reaches incongruent with visual cues (Kuang et al., 2015) and of decoupled arm and eye movements (Hawkins et al., 2013), suggesting that encoding in this region represents post-realignment directional information.

Areas representing eye movement direction

Monkey area LIP in the parietal cortex has been observed to be selective for the spatial location of the saccade target (Andersen et al. 1992; de Lafuente et al., 2015). The human homologue of monkey LIP has been suggested to be located in IPS (Schluppeck et al. 2005), although it is not yet clear exactly which of several observed maps in the parietal cortex correspond to human LIP (Hagler et al. 2007). These observations are also in line with results from human fMRI studies decoding the direction/target location (left vs. right) of upcoming saccades in middle and posterior IPS (Gallivan et al. 2011). Here, we have found that more anterior regions in the parietal cortex corresponding to SPLp and, at lower thresholds, SPLa and SPLr contained neural populations tuned to eye movement direction. These findings are in line with previous studies that found that neurons in medial posterior parietal cortex in the monkey are modulated by both eye direction and depth (Hadjidimitrakis et al., 2015; Breveglieri et al., 2012). Our findings suggest that these areas are not only coarsely sensitive to the difference between eye movements performed towards the left or right, but that the underlying neural populations show properties that are compatible with directional tuning.

Our searchlight-based RSA also identified FEF bilaterally (Anderson et al. 2012). This result is in line with previous findings revealing a topographic organization in FEF for saccade direction (Kastner et al. 2007). FEF has been suggested to be involved both in the allocation of attention and in the execution of eye movements (Corbetta et al. 1998; Moore and Armstrong, 2003; Murthy et al. 2001; Tanaka and Lisberger 2001). It is thus possible that the directional tuning we obtained in FEF is specific for eye movements, for the allocation of attention, or for both.

Overlapping regions for arm and eye movements

When superimposing the FDR-thresholded arm and eye direction maps, we were able to identify a region bilaterally in SPLp which contained directional tuning information for both effectors. These findings suggest that the posterior part of SPL is involved in the processing of directional information for both eye and arms. Our results are in line with monkey studies showing that areas homologous to or neighboring SPLp have a role in generalizing spatial information across effectors (Battaglia-Mayer et al. 2001, 2016; McGuire and Sabes 2011; de Lafuente et al. 2015). Further, SPLp has been shown to encode eye-centered, body-centered and hand-centered reference frames (Hadjidimitrakis et al., 2014), and is involved during both gaze and reach preparation (Breveglieri et al., 2014). Likewise, our results are in line with human fMRI studies showing that the direction (left vs right) of upcoming eye and arm movements can be decoded from left posterior IPS and bilateral middle IPS, adjacent to the overlapping regions observed in the current study, both within and across effectors (Gallivan et al. 2011).

As pointed out earlier, visual presentations of cues and corresponding performed movement were different for the saccade and for the reaching task. The same cue (an upward arrow) indicated a downward reach and an upward saccade. Thus, one might ask whether any obtained directional tuning was due to the processing of the visual cues rather than the direction of eye or arm movements. Several observations speak against such an interpretation. First, if our results were indeed due to the processing of visual cues, we should have obtained effector-independent directional tuning in early visual cortex, which was clearly not the case. Second, using the same set-up, but using auditory instead of visual cues, we obtained evidence for directional tuning for reach direction in similar regions as those reported in the current study in a group of 15 sighted and a group of 15 congenitally blind participants (Lingnau et al., 2012). Together, these observations are not in line with an interpretation of the results of the current study based on the processing of visual information.

Several lines of evidence support the existence of effector-nonspecific regions involved in integrating information in the parietal cortex: effector-specific activation in parietal cortex is linked with the representation of the spatial target and not exclusively with the preparation of movement, in line with the view that parietal cortex could have a role in the integration of spatial information across effectors (Medendorp et al. 2005; Beurze et al. 2007, 2009). In line with these findings, we were interested

in exploring the possibility that the cluster we obtained in the posterior SPL which showed directional tuning for both the arm and the eye could also represent information in an effector-independent way. This possibility seems likely given the observation of effector-independent decoding in nearby parietal areas (i.e. posterior and mid intraparietal sulcus; Gallivan et al., 2011). However, we did not find any evidence for a generalization of directional tuning across the two effectors. This could be due to at least two factors. First, the two tasks were run in separate sessions, which is likely to have reduced the chances to find generalization across effectors. Second, due to practical restrictions, eye and arm movements were performed on different planes and toward different spatial targets: towards a point on the screen for the saccade task, and towards a point on the reaching device for the arm movement task. This may have limited our chances to find a generalization of directional tuning across effectors.

4.5 Conclusion

We identified several parietal and frontal regions containing neuronal populations that were directionally tuned for arm or eye movements. Furthermore, we identified a region in the superior parietal cortex that shows directional tuning for both arm and eye movements, in line with the view that this region plays a role in integrating information between different effectors.

Acknowledgments

This research was supported by the Provincia Autonoma di Trento, and the Fondazione Cassa di Risparmio di Trento e Rovereto. We are grateful to Tjerk Gutteling for his comments on an earlier version of this manuscript.

DISCLOSURES

No conflicts of interest, financial or otherwise, are declared by the authors.

REFERENCES

Andersen RA, Brotchie PR, Mazzoni P. Evidence for the lateral intraparietal area as the parietal eye field. *Curr Opin Neurobiol* 2, 840–6, 1992.

Andersen RA, Cui H. Intention, action planning, and decision making in parietal-frontal circuits. *Neuron* 63, 568–83, 2009.

Anderson EJ, Jones DK, O'Gorman RL, Leemans A, Catani M, Husain M. Cortical network for gaze control in humans revealed using multimodal MRI. *Cereb Cortex* 22, 765–75, 2012.

Ariani, G., Wurm, M. F., & Lingnau, A. Decoding internally and externally driven movement plans. *Journal of Neuroscience*, *35*(42), 14160-14171, 2015.

Barany DA, Della-Maggiore V, Viswanathan S, Cieslak M, Grafton ST. Feature interactions enable decoding of sensorimotor transformations for goal-directed movement. *J Neurosci* 34, 6860–73, 2014.

Battaglia-Mayer A, Ferraina S, Genovesio A, Marconi B, Squatrito S, Molinari M, Lacquaniti F, Caminiti R. Eye-hand coordination during reaching. II. An analysis of the relationships between visuomanual signals in parietal cortex and parieto-frontal association projections. *Cereb Cortex* 11, 528–44, 2001.

Battaglia-Mayer A, Ferraina S, Mitsuda T, Marconi B, Genovesio A, Onorati P, Lacquaniti F, Caminiti R. Early coding of reaching in the parietooccipital cortex. *J Neurophysiol* 83, 2374–91, 2000.

Battaglia-Mayer A, Ferrari-Toniolo S, Visco-Comandini F, Archambault PS, Saberi-Moghadam S, Caminiti R. Impairment of online control of hand and eye movements in a monkey model of optic ataxia. *Cereb Cortex* 23, 2644–56, 2013.

Battaglia-Mayer A, Babicola L, Satta E. Parieto-frontal gradients and domains underlying eye and hand operations in the action space. *Neuroscience*, 334, 76–92, 2016.

Benjamini Y, Yekutieli D. The control of the false discovery rate in multiple testing under dependency. Ann Stat 1165–1188. 2001.

Beurze SM, de Lange FP, Toni I, Medendorp WP. Spatial and effector processing in the human parietofrontal network for reaches and saccades. *J Neurophysiol* 101, 3053–62, 2009.

Beurze SM, de Lange FP, Toni I, Medendorp WP. Integration of target and effector information in the human brain during reach planning. *J Neurophysiol* 97, 188–99, 2007.

Brainard DH. The Psychophysics Toolbox. *Spat Vis* 10, 433–436, 1997.

Breveglieri R, Hadjidimitrakis K, Bosco A, Sabatini SP, Galletti C, Fattori P. Eye Position Encoding in Three-Dimensional Space: Integration of Version and Vergence Signals in the Medial Posterior Parietal Cortex. *J Neurosci* 32, 159–169, 2012.

Breveglieri R, Galletti C, Dal Bò G, Hadjidimitrakis K, Fattori P. Multiple Aspects of Neural Activity during Reaching Preparation in the Medial Posterior Parietal Area V6A. J Cog Neurosci 26, 878–895, 2014.

644 **Breveglieri R, De Vitis M, Bosco A, Galletti C, Fattori P.** Interplay Between Grip
645 and Vision in the Monkey Medial Parietal Lobe. *Cereb Cortex* 28:2028–2042,
646 2017.

647 **Bruce CJ, Goldberg ME, Bushnell MC, Stanton GB.** Primate frontal eye fields. II.
648 Physiological and anatomical correlates of electrically evoked eye movements. *J*
649 *Neurophysiol* 54, 714–34, 1985.

650 **Caminiti R, Johnson PB, Galli C, Ferraina S, Burnod Y.** Making arm movements
651 within different parts of space: The premotor and motor cortical representation of
652 a coordinate system for reaching to visual targets. J Neurosci 11, 1182-1197,
653 1991.

654 **Connolly JD, Andersen RA, Goodale MA.** FMRI evidence for a "parietal reach
655 region" in the human brain. *Exp brain Res* 153, 140–5, 2003.

656 **Corbetta M, Akbudak E, Conturo TE, Snyder AZ, Ollinger JM, Drury HA, Lin-**
657 **enweber MR, Petersen SE, Raichle ME, Van Essen DC, Shulman GL.** A
658 common network of functional areas for attention and eye movements. *Neuron*
659 21, 761–73, 1998.

660 **de Lafuente V, Jazayeri M, Shadlen MN.** Representation of accumulating evidence
661 for a decision in two parietal areas. J Neurosci 35:4306-4318, 2015.

662 **Eisenberg M, Shmuelof L, Vaadia E, Zohary E.** Functional organization of human
663 motor cortex: directional selectivity for movement. *J Neurosci* 30, 8897–905,
664 2010.

665 **Fabbri S, Caramazza A, Lingnau A.** Distributed sensitivity for movement ampli-
666 tude in directionally-tuned neuronal populations. *J Neurophysiol* 107, 1845–
667 1856, 2012.

668 **Fabbri S, Caramazza A, Lingnau A.** Tuning curves for movement direction in the
669 human visuomotor system. *J Neurosci* 30, 13488–98, 2010.

670 **Fabbri S, Strnad L, Caramazza A, Lingnau A.** Overlapping representations for
671 grip type and reach direction. *Neuroimage* 94, 138–46, 2014.

672 **Fattori P, Breveglieri R, Marzocchi N, Filippini D, Bosco A, Galletti C**. Hand Ori-
673 entation during Reach-to-Grasp Movements Modulates Neuronal Activity in the
674 Medial Posterior Parietal Area V6A. *J Neurosci* 29:1928–1936, 2009.

675 **Fischl B, Sereno MI, Tootell RB, Dale AM.** High-resolution intersubject averaging
676 and a coordinate system for the cortical surface. *Hum Brain Mapp* 8, 272–84,
677 1999.

678 **Friston KJ, Fletcher P, Josephs, O, Holmes A, Rugg MD, Turner R.** Event-related
679 fMRI: characterizing differential responses. *Neuroimage* 7, 30–40, 1998.

680 **Gallivan JP, McLean DA, Smith FW, Culham JC.** Decoding effector-dependent
681 and effector-independent movement intentions from human parieto-frontal brain
682 activity. *J Neurosci* 31, 17149–68, 2011.

683 **Georgopoulos AP, Kalaska JF, Caminiti R, Massey JT.** On the relations between
684 the direction of two-dimensional arm movements and cell discharge in primate
685 motor cortex. *J Neurosci* 2, 1527–37, 1982.

Georgopoulos AP, Schwartz AB, Kettner RE. Neuronal population coding of movement direction. *Science* 233, 1416–9, 1986.

Gnadt JW, Andersen RA. Memory related motor planning activity in posterior parietal cortex of macaque. *Exp brain Res* 70, 216–20, 1988.

Hadjidimitrakis K, Bertozzi F, Breveglieri R. Fattori P, & Galletti C. Body-Centered, Mixed, but not Hand-Centered Coding of Visual Targets in the Medial Posterior Parietal Cortex During Reaches in 3D Space. *Cereb Cortex 24*(12), 3209–3220, 2014.

Hadjidimitrakis K, Dal Bò G, Breveglieri R, Galletti C, & Fattori P. Overlapping representations for reach depth and direction in caudal superior parietal lobule of macaques. *J Neurophysiol*, *114*(4), 2340–2352, 2015.

Hagler DJ, Riecke L, Sereno MI. Parietal and superior frontal visuospatial maps activated by pointing and saccades. *Neuroimage* 35, 1562–77, 2007.

Hawkins KM, Sayegh P, Yan X, Crawford JD, & Sergio LE. Neural activity in superior parietal cortex during rule-based visual-motor transformations. *J Cog Neurosci*, *25*(3), 436-454, 2013.

Haxby JV, Gobbini MI, Furey ML, Ishai A, Schouten JL, Pietrini P. Distributed and overlapping representations of faces and objects in ventral temporal cortex. *Science* 293, 2425–30, 2001.

Johnson PB, Ferraina S, Bianchi L, Caminiti R. Cortical Networks for Visual Reaching: Physiological and Anatomical Organization of Frontal and Parietal Lobe Arm Regions. *Cereb Cortex* 6, 102–119, 1996.

Kastner S, DeSimone K, Konen CS, Szczepanski SM, Weiner KS, Schneider KA. Topographic maps in human frontal cortex revealed in memory-guided saccade and spatial working-memory tasks. *J Neurophysiol* 97, 3494–507, 2007.

Kriegeskorte N, Goebel R, Bandettini P. Information-based functional brain mapping. *Proc Natl Acad Sci U.S.A.* 103, 3863–8, 2006.

Kriegeskorte N, Mur M, Bandettini P. Representational similarity analysis - connecting the branches of systems neuroscience. *Front Syst Neurosci* 2, 4, 2008.

Kuang S, Morel P, Gail A. Planning Movements in Visual and Physical Space in Monkey Posterior Parietal Cortex. *Cereb Cortex , 26*(2), 731-747, 2015.

Leoné FTM, Heed T, Toni I, Medendorp WP. Understanding effector selectivity in human posterior parietal cortex by combining information patterns and activation measures. *J Neurosci* 34, 7102–12, 2014.

Levy I, Schluppeck D, Heeger DJ, Glimcher PW. Specificity of human cortical areas for reaches and saccades. *J Neurosci* 27, 4687–96, 2007.

Lingnau A, Strnad L, He C, Fabbri S, Han Z, Bi Y, Caramazza A. Cross-Modal Plasticity Preserves Functional Specialization in Posterior Parietal Cortex. *Cereb Cortex*, 2012.

Mahan MY, Georgopoulos AP. Motor directional tuning across brain areas: directional resonance and the role of inhibition for directional accuracy. Front. Neural Circuits 7, 92, 2013.

McGuire LMM, Sabes PN. Heterogeneous representations in the superior parietal

lobule are common across reaches to visual and proprioceptive targets. *J Neurosci* 31, 6661–73, 2011

Medendorp WP, Goltz HC, Crawford JD, Vilis T. Integration of target and effector information in human posterior parietal cortex for the planning of action. *J Neurophysiol* 93, 954–62, 2005.

Monaco S, Cavina-Pratesi C, Sedda A, Fattori P, Galletti C, Culham JC. Functional magnetic resonance adaptation reveals the involvement of the dorsomedial stream in hand orientation for grasping. J Neurophysiol 106, 2248–2263, 2011.

Moore T, Armstrong KM. Selective gating of visual signals by microstimulation of frontal cortex. *Nature* 421, 370–3, 2003.

Murthy A, Thompson KG, Schall JD. Dynamic dissociation of visual selection from saccade programming in frontal eye field. *J Neurophysiol* 86, 2634–7, 2001.

Orban GA. Functional definitions of parietal areas in human and non-human primates. Proc Biol Sci 283, 2016.

Pelli DG. The VideoToolbox software for visual psychophysics: transforming numbers into movies. *Spat Vis* 10, 437–442, 1997.

Ritchie, J. B., Bracci, S., & de Beeck, H. O. Avoiding illusory effects in representational similarity analysis: What (not) to do with the diagonal. *Neuroimage*, 148, 197-200, 2017

Scherberger H, Andersen RA. Target selection signals for arm reaching in the posterior parietal cortex. *J Neurosci* 27, 2001–12, 2007.

Schluppeck D, Glimcher P, Heeger DJ. Topographic organization for delayed saccades in human posterior parietal cortex. *J Neurophysiol* 94, 1372–84, 2005.

Schwarzbach J. A simple framework (ASF) for behavioral and neuroimaging experiments based on the psychophysics toolbox for MATLAB. *Behav Res Methods* 43, 1194–201, 2011.

Sereno MI, Pitzalis S, Martinez A. Mapping of contralateral space in retinotopic coordinates by a parietal cortical area in humans. *Science* 294, 1350–4, 2001.

Snyder LH, Batista AP, Andersen RA. Coding of intention in the posterior parietal cortex. *Nature* 386, 167–70, 1997.

Stevenson IH, Cherian A, London BM, Sachs NA, Lindberg E, Reimer J, Slutzky MW, Hatsopoulos NG, Miller LE, Kording KP. Statistical assessment of the stability of neural movement representations. *J Neurophysiol* 106, 764–74, 2011

Tanaka M, Lisberger SG. Regulation of the gain of visually guided smooth-pursuit eye movements by frontal cortex. *Nature* 409, 191–4, 2001.

Zaitsev M, Hennig J, Speck O. Point spread function mapping with parallel imaging techniques and high acceleration factors: fast, robust, and flexible method for echo-planar imaging distortion correction. *Magn Reson Med* 52, 1156–66, 2004

Zeng H, Constable RT. Image distortion correction in EPI: comparison of field mapping with point spread function mapping. *Magn Reson Med* 48, 137–146, 2002.

771 **Zhang M, Barash S.** Neuronal switching of sensorimotor transformations for anti-
772 saccades. *Nature* 408, 971–5, 2000.